CSIRO PUBLISHING
www.publish.csiro.au/journals/eg *Exploration Geophysics*, 2009, **40**, 173–183

Spatially constrained inversion for quasi 3D modelling of airborne electromagnetic data – an application for environmental assessment in the Lower Murray Region of South Australia

Andrea Viezzoli[1,3] Esben Auken[1] Tim Munday[2]

[1]Department of Earth Sciences, University of Aarhus, Høegh-Gulbergs Gade 2, Aarhus C 8000, Denmark.
[2]CSIRO, ARRC, 26 Dick Perry Avenue, Kensington, WA 6151, Australia.
[3]Corresponding author. Email: andrea.viezzoli@geo.au.dk

Abstract. We present an application of spatially constrained inversion (SCI) of SkyTEM (airborne electromagnetic) data for defining spatial patterns of salinisation in the Bookpurnong irrigation area located in the lower Murray Basin of South Australia. SCI uses Delaunay triangulation to set 3D constraints between neighbouring soundings, taking advantage of the spatial coherency that may be present in the dataset. Conductivity information for individual soundings is linked through the spatial constraints, from well determined parameters to locally poorly determined parameters. For the survey presented here, SCI generated maps detail the spatial variability of floodplain salinisation, the extent of floodplain sediments influenced by lateral recharge and flushing along stretches of the Murray River, and the variable quality of groundwater in deeper semi-confined aquifers of the Murray Group. Available borehole and other ancillary information, such as vegetation density and health patterns, match the observed conductivity variations seen in the SCI results, even at the very near surface (≈2m depth). The SCI provides more accurate and spatially consistent results compared with those from single site inversions. They are also more uniform and detailed than maps obtained with single point Layered Earth Inversions or a laterally constrained inversion. In this example, the SCI provided reliable quasi 3D modelling, that confirmed and improved the hydrogeological knowledge of the area, indicating that the technique would have application with helicopter electromagnetic data in similar settings throughout the lower Murray Basin of Australia.

Key words: airborne electromagnetic, quasi 3D, salinisation, SkyTEM, spatially constrained inversion.

Introduction

Airborne electromagnetic (AEM) data acquired for exploration or environmental applications are commonly modelled using algorithms such as conductivity depth transforms (CDTs) or layered earth inversions (LEIs) that assume a 1D earth (Wolfgram and Karlik, 1995; Sattel, 2005). To date, full 2.5D or 3D inversion of AEM data remains limited, and in many respects unrealistic and unnecessary particularly for hydrogeological investigations in many Australian basins. In such contexts the assumption that the subsurface can be represented as a series of horizontal layers holds reasonably well, particularly at the scale of the footprint of most AEM systems (Sattel, 1998; Lane, 2000). The 1D model assumption is also legitimate in sub-horizontal, layered sedimentary areas where it produces results that are only slightly distorted by 2D or 3D effects such as might be induced by faults, fractures, or other geological phenomena (Newman et al., 1987; Sengpiel and Siemon, 2000; Auken et al., 2005).

There are different inversion strategies within the 1D forward assumptions. The output models can be simply stitched together (Auken et al., 2003; Huang and Fraser, 2003), an approach that often results in abrupt variations in neighbouring models, because of noisy data and model ambiguity. Models with smooth lateral variations, typical of the sedimentary areas, can be achieved either by working in the data domain, or in the model domain. In the first approach, raw data are smoothed before inversion, resulting in a loss of lateral resolution. In the second approach, constraints are applied between adjacent output models during the inversions. An increasingly popular example is the laterally constrained inversion (LCI) (Auken and Christiansen, 2004). The LCI is profile-oriented, in the sense that it aims to produce a continuum of model parameters along the flight line. However, it does not create any connection between neighbouring lines. Features that are perpendicular to lines benefit only partially from in-line constraints or averaging, as no information is passed between adjacent lines. This means that profile oriented techniques like the LCI, favour structures following the flight (or profile) direction. Images produced using these methods are often characterised by some lineation following the fight paths. In order to avoid these artefacts, and to produce a quasi 3D model, the concepts developed with the LCI of applying lateral constraints along a flight line, were extended to incorporate constraints from both along and across flight lines and incorporated into the spatially constrained inversion (SCI) (Viezzoli et al., 2008).

Methodology

The mechanisms of the SCI are explained in more detail in Viezzoli et al. (2008). It is a least-squares inversion of a layered earth regularised through spatial constraints, which produce smooth lateral transitions. Information (including a

 10.1071/EG08027 0812-3985/09/020173

priori information) migrates between neighbouring soundings through the constraints. The constraints are set up to reflect the expected local geological variations in the area. Both the data and the lateral constraints are part of the inversion, which therefore results in output models that are a balance between the data and the constraints. Model parameters that exert little influence on the data will be controlled more by the constraints, and vice versa. In formulae, the inversion problem is defined as

$$\begin{bmatrix} \mathbf{G} \\ \mathbf{R} \end{bmatrix} \mathrm{g}\delta\mathbf{m}_{\mathrm{true}} = \begin{bmatrix} \delta\mathbf{d}_{\mathrm{obs}} \\ \delta\mathbf{r} \end{bmatrix} + \begin{bmatrix} \mathbf{e}_{\mathrm{obs}} \\ \mathbf{e}_{\mathbf{r}} \end{bmatrix}. \quad (1)$$

The Jacobian matrix, **G** contains the partial derivatives of the mapping (data information); the roughening matrix **R** describes the spatial constraints. The vector $\delta\mathbf{d}_{\mathrm{obs}}$ is the difference between the observed data and reference model, $\mathbf{e}_{\mathrm{obs}}$ is the error on the observed data, $\delta\mathbf{r}$ are the constraints and $\mathbf{e}_{\mathbf{r}}$ is the error on the constraints, with 0 as expected value. The difference between LCI and SCI lies in the covariance matrix **R**, which in the first case establishes links between soundings only along profiles, in the second case also across them. The spatial constraints can be set between any model parameter (Auken and Christiansen, 2004). Our usual approach is to constrain layer resistivities and layer boundaries (either by inverting from depth below the surface or by elevation).

The implementation of the SCI poses a few issues that need to be addressed. The first step for constraining soundings that are scattered over an area is to choose a strategy for connecting these points. Such connections need to be repeatable, not arbitrary, and adapt, as much as possible, to the spatial patterns present in the dataset.

In our approach we use Delaunay triangulation (Delaunay, 1934). Delaunay triangles vary in dimension according to local data density. They adapt to the dataset so that they are small and numerous in high-density areas, and large and fewer in low-density areas. The number of connections to each sounding is not set arbitrarily, but depends on data density and distribution. In AEM surveys, Delaunay triangulation always connects adjacent survey lines, which is the preliminary condition for breaking down the preference for line orientation in the data. Therefore, we choose to set the constraint between the soundings connected by Delaunay triangles (also known as the nearest neighbours, see Figure 1). The result is a continuum of interconnected soundings, each of which is only constrained to its nearest neighbour. Information spreads horizontally between nearest neighbours, and then to the whole dataset. The strength of the constraints that result in a particular layer continuity is determined empirically.

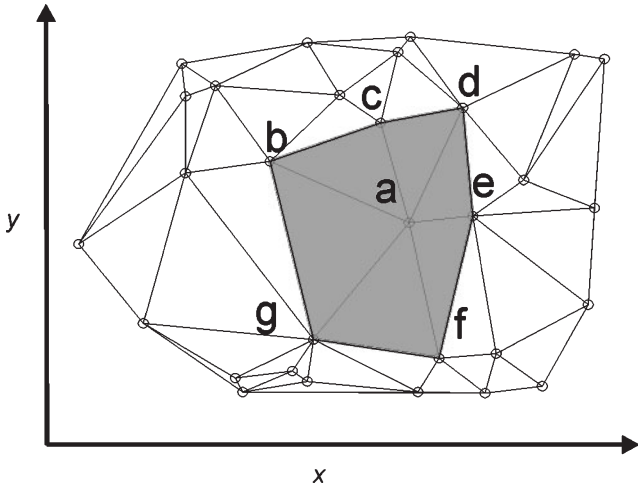

Fig. 1. Delaunay triangulation of random generated points on a plane. Points **b** to **g** are nearest neighbours of point **a**.

In the present formulation, the SCI uses non-sparse matrix operators. This requires typical datasets of thousands of soundings to be divided into smaller subsets. Each subset is then inverted with spatial constraints, as a unit. We produce the cells using the pre-constructed Delaunay triangles. We select a starting point (the location of a transient electromagnetic sounding) randomly, and then identify its nearest neighbours, as defined above. They produce an outer border around the starting point. Then we identify the nearest neighbours to each of the points along the border. This way the cell is expanded to the next order of nearest neighbours. We keep expanding the cell in a similar fashion until a predefined number of points are included in the cell. After the first cell has been built, the second one is obtained by iterative nearest neighbours expansions around one of the points along the outer border of the first cell, and so on, until all data points are included in a cell. We then expand the cells around their borders, one more order of nearest neighbours. In this way we create a double overlap between neighbouring cells. This overlap region is essential for the migration of information between cells. The total number of cells is divided into as many CPUs as available, and the SCI is run in parallel. In this first run information migrates from the centre of the cells to the overlapping region along their borders (see Figure 2*a*). The results of this first run are used as a priori information or as starting models for a second and final SCI run. The a priori information inserted along the overlapping region brings along information coming from the neighbouring cells, which spreads back towards the centre of each cell (see Figure 2*b*).

Field example: Bookpurnong Irrigation District, SA

The SCI can be applied to different data types. Here, we present a case study using airborne transient electromagnetic (TEM) soundings collected with the SkyTEM time domain helicopter EM system (Sørensen and Auken, 2004) in early September 2006.

Survey area

The survey was conducted over the Bookpurnong and Clarks floodplains adjacent to the Murray River in the Bookpurnong Irrigation District of the Riverland region of South Australia (Figure 3). The area, located ~12 km upstream from the township of Loxton, has been the focus of trials to manage a marked decline in tree health that has been observed along the River Murray in South Australia and elsewhere, largely in response to floodplain salinisation from groundwater discharge in combination with the decrease in flooding frequency, permanent weir pool levels and the recent drought (Jolly et al., 2006; White et al., 2006).

The study area at Bookpurnong is characterised by a semi-arid climate typical of lower River Murray in South Australia, and it is typically vegetated by a mixture of river red gums (*Eucalyptus camaldulensis*), black box (*Eucalyptus largiflorens*), river cooba (*Acacia stenophylla*) and lignum (*Muehlenbeckia florenta*). Understorey species are dominated by chenopod species (White et al., 2006). The Bookpurnong floodplain has become significantly degraded largely in response to salinisation due to groundwater discharge, but it has also experienced a significant increase in vegetation dieback over the past 5 years.

Several floodplain management options are being explored at Bookpurnong aimed at trialling and comparing their effectiveness for rejuvenating red gum, black box, cooba, and understorey

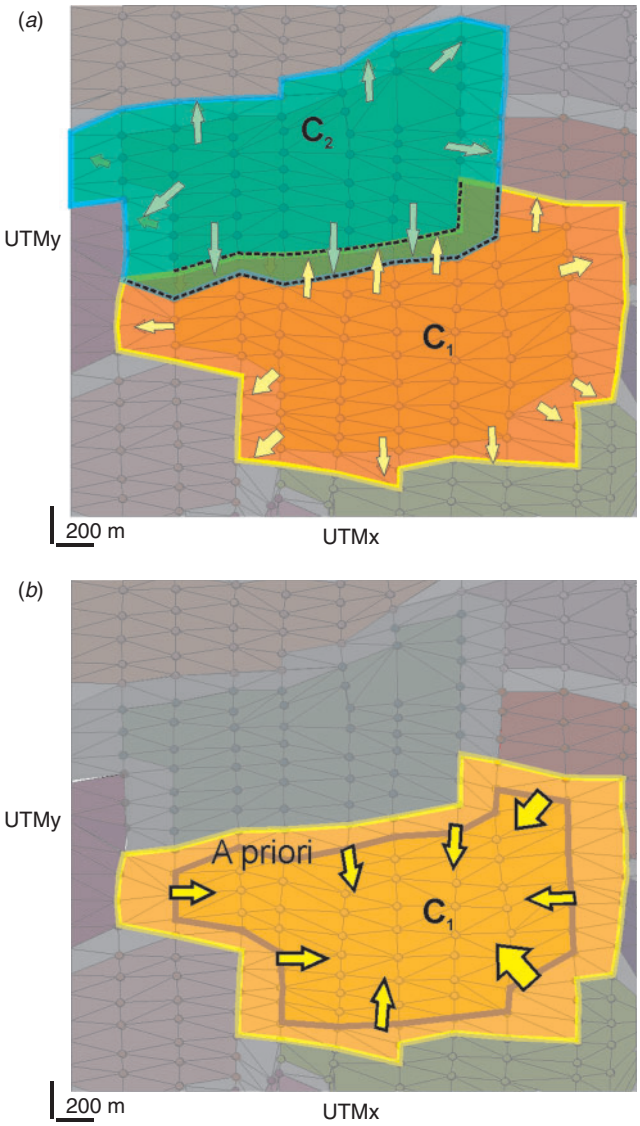

Fig. 2. (*a*) Schematic of information flow between cells in first spatially constrained inversion (SCI) run. (*b*) Schematic of information flow between cells the second SCI run.

vegetation communities. They include managed flooding projects being undertaken in several priority areas, and the deployment and operation of a salt interception scheme (SIS) aimed at lowering groundwater levels through pumping. The Bookpurnong SIS, which has been in operation for more than 8 months, has production wells located on Clark's floodplain and along the bordering highlands, which are designed to intercept saline groundwater that flows from the highland irrigation area into the floodplain aquifer. Before the SIS was operational the irrigation-induced groundwater mound forced the naturally saline groundwater onto the floodplain at a relatively high flow rate, thereby increasing soil salinity in the root zone of the floodplain woodlands.

The SkyTEM survey was undertaken as part of a larger study that also included an investigation of ground-based (EM 31 and NanoTEM), river-borne (NanoTEM) and airborne FDHEM (RESOLVE) measurements. Together with borehole hydrological information, the project was directed at producing a more complete near-surface hydrological model of the area, and at monitoring the results of the remediation schemes set in place (White et al., 2006).

Fig. 3. Location of Bookpurnong SkyTEM Survey, in the Lower Murray Basin.

Hydrogeology

The floodplain at Bookpurnong occupies a relatively narrow stretch of the Murray River valley incised through a Late Cainozoic succession consisting of the Blanchetown Clay and Loxton-Parilla Formations (Brown and Stephenson, 1991). These are mantled by Pleistocene aeolian sands of the Woorinen Formation (represented schematically in Figure 4). The Bookpurnong floodplain has a hydrogeology typical of the Lower Murray region, with sediments on the floodplain consisting of the Coonambidgal Clay (ranging from 3 to 7 m thick), underlain by the Monoman Formation which consists of a fine to coarse sand with varying amounts of silt and clay, up to 10 m thick in this area. Sediments of the Loxton-Parilla sands, which can be up to 35 m thick, outcrop in the cliffs adjacent to the floodplain. The whole area is underlain by the Tertiary marine sediments of the Bookpurnong Beds and the Murray Group Formation, the latter consisting mainly of limestone with marl and clay units (Brown and Stephenson, 1991). The Bookpurnong Beds act as an aquitard basement to the shallow, unconfined aquifer that encompasses the Monoman Formation and Loxton Sands. Saline groundwater lies beneath the floodplain, within the Monoman Formation, with the depth to watertable ranging from 2 to 4 m below the surface. The majority of the floodplain groundwater has an approximate conductivity of 5 $S.m^{-1}$, with a flushed zone known to occur along the river in some places. It is worth noting that the physiological limit for water uptake in this environment is 3 $S.m^{-1}$ by river red gums and 5.5 $S.m^{-1}$ by black box trees (Overton and Jolly, 2004). Hydrogeologically, the river is the natural sink or discharge point for the regional groundwater within the Loxton–Bookpurnong area.

Excess recharge from the Bookpurnong Irrigation District has led to the formation of a groundwater mound (illustrated schematically in Figure 4), which displaces saline groundwater towards the floodplain and has led to increased waterlogging and salinisation on the floodplain, and localised groundwater seepage at the break of slope adjacent to the cliffs.

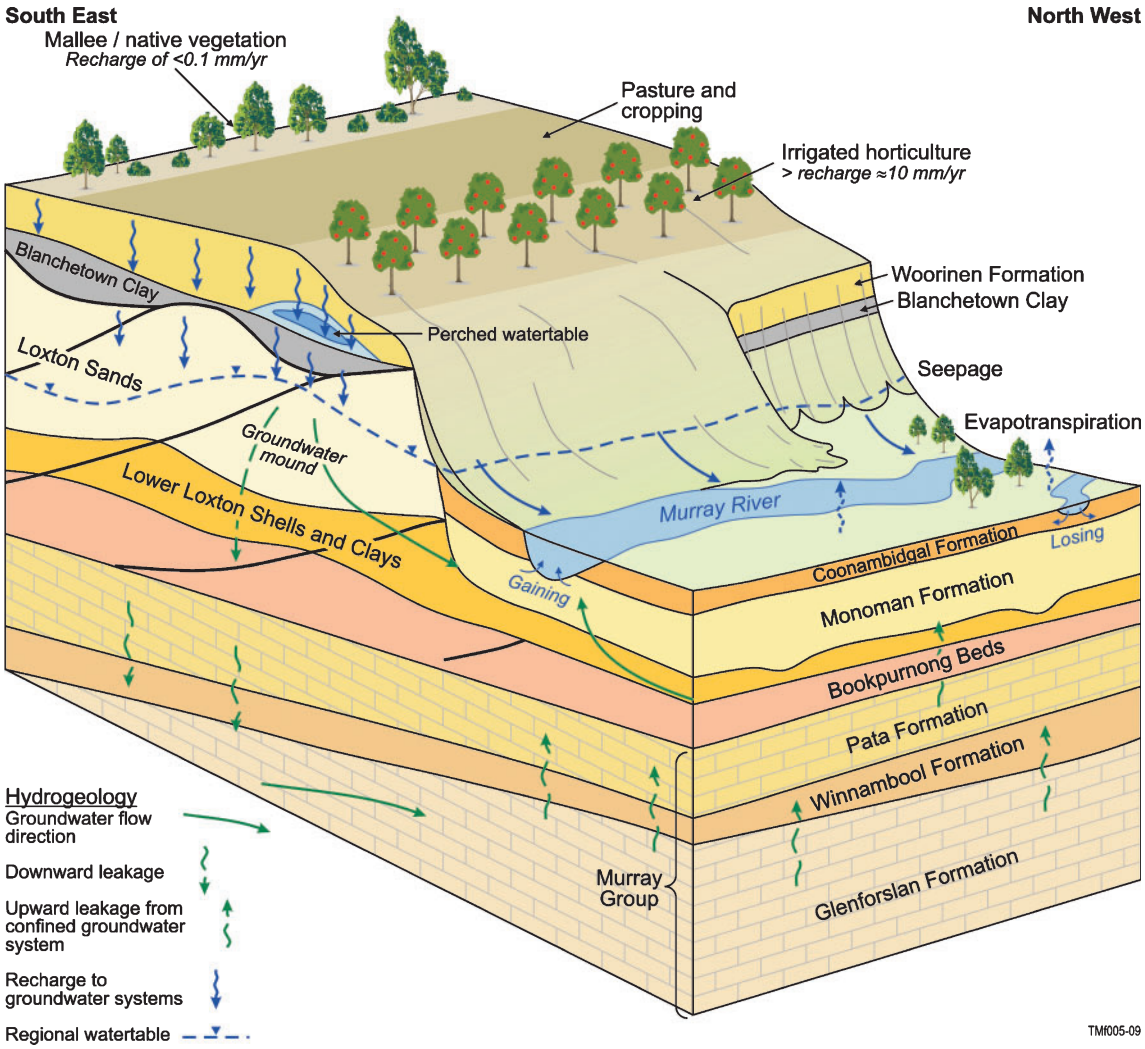

Fig. 4. Schematic of the hydrogeology across the Bookpurnong study area.

Geophysical investigations

Several hydrogeophysical investigations have been undertaken over the Bookpurnong floodplain and in the Murray River itself, linked to the floodplain management trials mentioned earlier. These have involved spatio-temporal studies of floodplain salinity using a Geonics EM31 (see Berens et al., 2007), an examination of the riverbed salt loads using the 'in-stream' NanoTEM (see Berens and Hatch, 2006), and an investigation of the spatial variability of salt stored in the near surface using the RESOLVE frequency-domain helicopter EM system (see Munday et al., 2005).

The present analysis is based on data from a SkyTEM survey, which was carried out over Bookpurnong to investigate its merits for examining surface water – groundwater interactions in these highly saline environments, where low-powered EM systems have limited depths of investigation.

The SkyTEM time domain EM system is carried as a sling load towed beneath the helicopter at a nominal survey height of 30 m (Sørensen and Auken, 2004). Nominal survey altitude of the transmitter in the Bookpurnong survey was ~60 m. SkyTEM is capable of operating in a dual transmitter mode. In the low-moment mode, a low-current, high base frequency and fast switch-off provides early-time data for shallow imaging. By contrast, when in high-moment mode, a higher current and a lower base frequency provide late-time data for deeper imaging. The two modes can be run sequentially during a survey, and for the Bookpurnong survey the system was used in the combined, or dual, mode.

Twenty-nine lines of SkyTEM data spaced every 100 m were acquired over the floodplain in a similar orientation to a previous survey undertaken with the RESOLVE FDHEM system (see Munday et al., 2005). One line was collected perpendicular to the primary flight line orientation (see Figure 5*a*). The survey area is ~7 × 3 km, with the sounding spacing along line varying between 35 and 45 m.

The SCI was carried out with a 4-layer model started from a homogeneous half space of 20 Ω.m. The number of layers chosen was based on the results of a fast, multilayered 1D inversion carried out beforehand. The expected lateral variations in the geology suggested the application of moderately tight spatial constraints. For a more detailed discussion on constraint strength the reader is referred to Auken and Christiansen (2004).

SCI results

The results of the SCI applied to the Bookpurnong SkyTEM data are presented in Figure 5*b–e* as average interval resistivity maps for 2 m depth increments, from surface to 8 m below the ground surface. The dashed line superimposed on some of the images represents the transition zone between tree-covered and less densely vegetated sections of the floodplain. This zone was defined from an interpretation of high-resolution false colour infrared aerial photography covering the area.

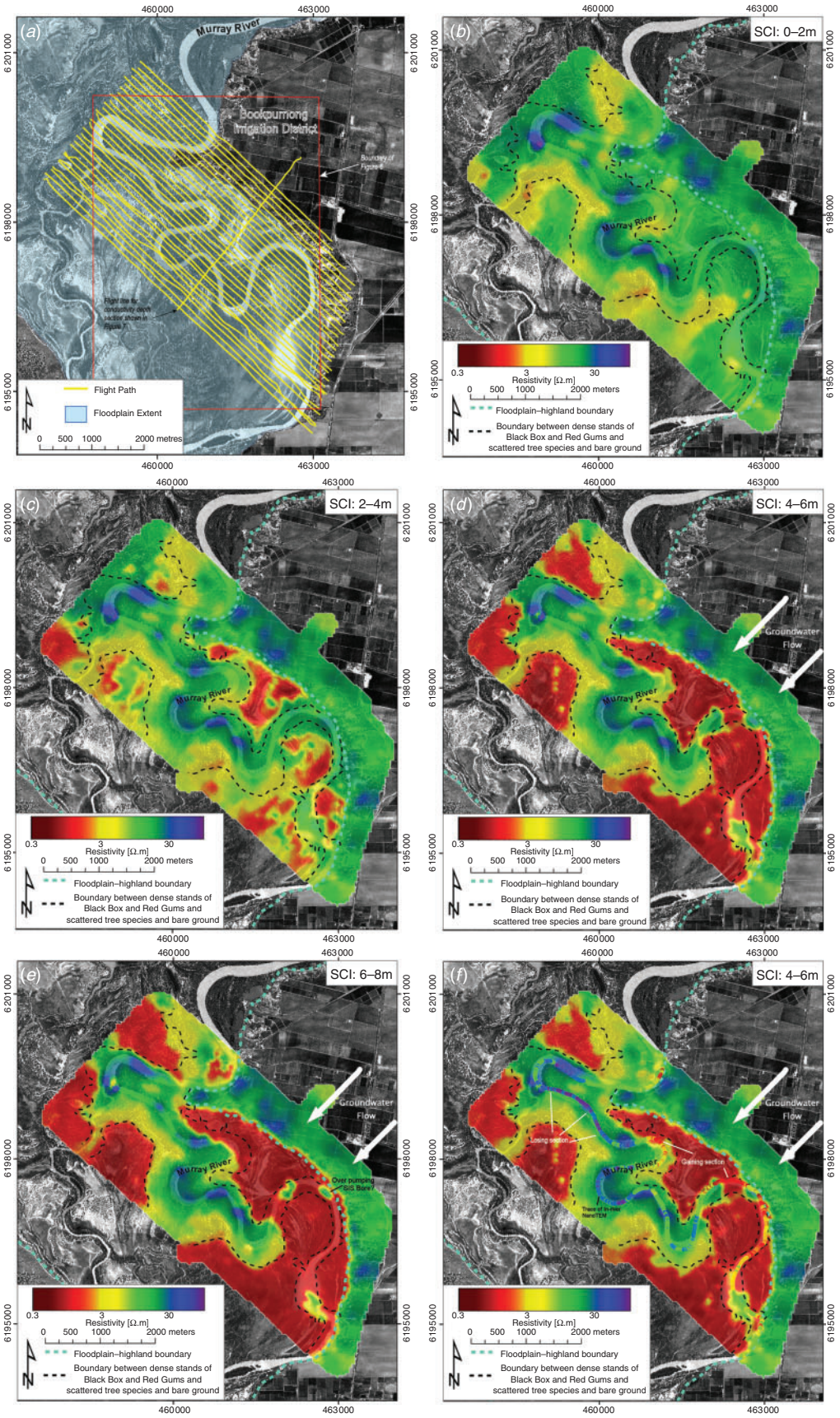

Fig. 5. (*a*) Aerial photo of the Bookpurnong area, with SkyTEM flight lines in yellow. The dashed black line marks a boundary between low density tree cover and the presence of thicker stands of red gum and black box tree species. The red box delimits the boundary of the area shown in Figure 6. Average resistivity maps obtained with spatially constrained inversion (SCI), for depth intervals of (*b*) 0–2 m, (*c*) 2–4 m, (*d*) 4–6 m, (*e*) 6–8 m. (*f*) Comparison between SCI 4–6 m and in-river NanoTEM data.

Figure 5*b–e* show a meandering, well defined resistive zone which follows the path of the Murray River. This resistive zone is most pronounced in the central and northern portion of the interval resistivity maps and reflects losing stretches of the river, where fresh river water is laterally recharging and flushing the floodplain sediments of salts. The process is also illustrated in Figure 4. The flushed zone extends up to ~400 m west of the river, and ~200 m east of it.

Resistive features shown in the resistivity images at the root zone depth intervals (2–4 m and 4–6 m) correspond well with the observed transition between the sparsely vegetated floodplain and the presence of trees including red gums and black box species.

An extensive conductive area, at a depth of ≥6 m occupies almost the entire floodplain between the river and the highlands. This represents part of the regional saline groundwater system which at Bookpurnong discharges at the floodplain-highlands boundary in response to increased upward head linked to the mounding of groundwater. In the Bookpurnong irrigation area, the development of a groundwater mound has resulted from increased recharge associated with irrigation (shown schematically in Figure 4). Available bore data indicates that it has a groundwater head almost 10 m above river pool level and is ~0.5 km from the floodplain-highland boundary.

In the south-eastern portion of the river, where it meanders close to the highland-floodplain boundary, the resistive flushed zone areas are noticeably smaller or non-existent compared with the central and northern sections of the river. In these areas, in a stretch referred to as a *gaining reach*, saline groundwater discharges into the river. Numerical modelling has indicated that before salt interception, around 100 tonnes of salt discharged into the river along the 18 km Bookpurnong river reach per day, with a significant portion emanating from the river reach in the south-eastern portion of the survey area (Yan et al., 2005). The Bookpurnong SIS was implemented to reduce this discharge by lowering the groundwater in this area. The SIS scheme began operation in July 2005, over a year before the SkyTEM survey. Interestingly, a localised resistive feature coincident with a SIS bore (identified by the black arrow in Figure 5*e*) may imply that the SIS is over-pumping at this bore, lowering the groundwater and drawing fresh river water into the sediments of the river bed in its vicinity.

We have examined the SCI outputs against in-river NanoTEM data and available bore-water EC data for the floodplain. As previously mentioned, an in-river NanoTEM survey had been carried out in 2004 (Berens and Hatch 2005), with the aim of measuring the resistivity of the sediments at river bottom, in order to differentiate between gaining and loosing stretches of the river. Figure 5*f* shows the good agreement between the SCI results at 4–6 m depth (the average river depth in the area), and the results obtained with NanoTEM. Figure 6 shows a subset of the 4–6 m SCI average resistivity map for an area over Clark's floodplain. Groundwater salinity data extracted from bores are superimposed on these interval resistivity data (coloured dots).

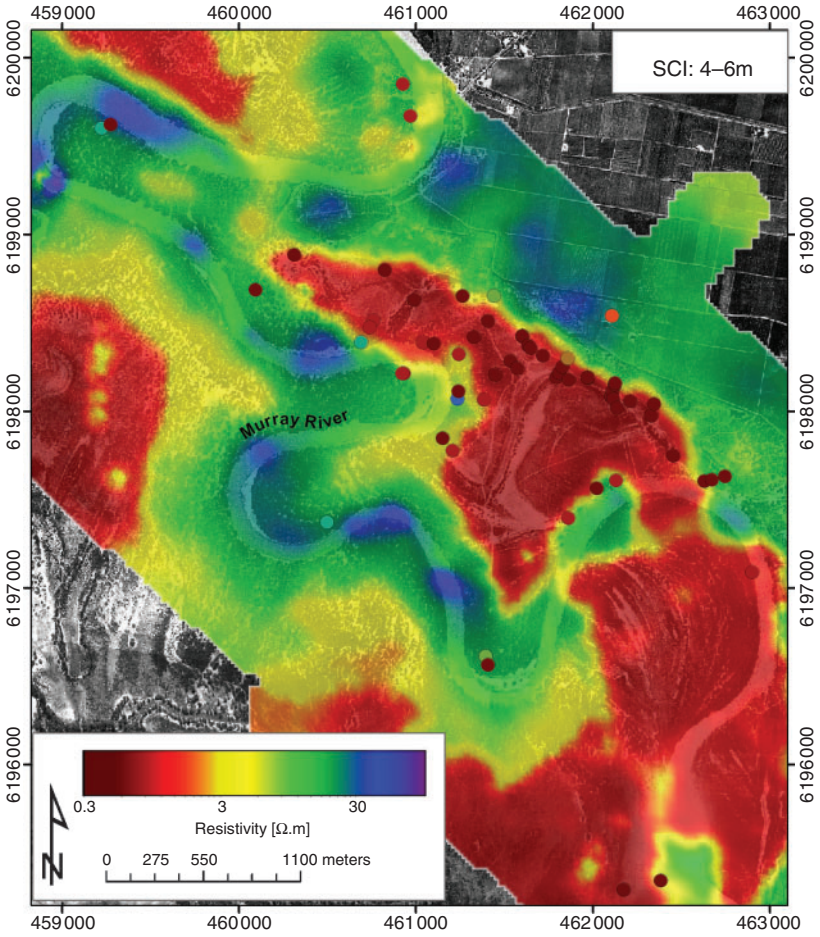

Fig. 6. Sub-set of the interval resistivity depth map for 4–6m with borehole electrical conductivity values overlain (dots). The spatially constrained inversion (SCI) map shows a good correlation with the groundwater conductivity.

Overall, there is good spatial agreement between SCI results and bore data, suggesting that the variability in the observed ground conductivity from the SCI, at the depth shown, is predominantly related to variations in groundwater quality rather than material type.

An elucidation of the hydrogeology is effectively developed from an interpretation of a resistivity depth section or profile (see Figure 7) for the flight line flown in the SE–NW direction, perpendicular to the highland-floodplain boundary (see Figure 5*a*). A resistive layer (fresh irrigation water) overlies a conductive saline groundwater system, with increased hydraulic pressure from the presence of a groundwater mound under the highlands (developed from excessive recharge of fresh irrigation water), causing discharge on the foot slopes of the cliffs, with salt accession and salinisation of the alluvial environment occurring primarily through evapotranspiration. A very shallow saline groundwater system occurs in the area north and east of the river with a fresh river water flushed zone extending to the west. The sub-surface relationships between water quality and inter-aquifer behaviour, as they occur across the floodplain-highland boundary are also illustrated in the section. The saline groundwater system (up to 80 m thick) overlies a more resistive layer, which starts appearing at depths >80 m. This most likely represents a change in the water quality present in the limestone aquifers of the Murray Group (Brown and Stephenson, 1991) (see Figure 4). The irregular boundary at the base of the conductive zone sits in the Mannum Formation and may be related to inter-aquifer leakage with groundwater of

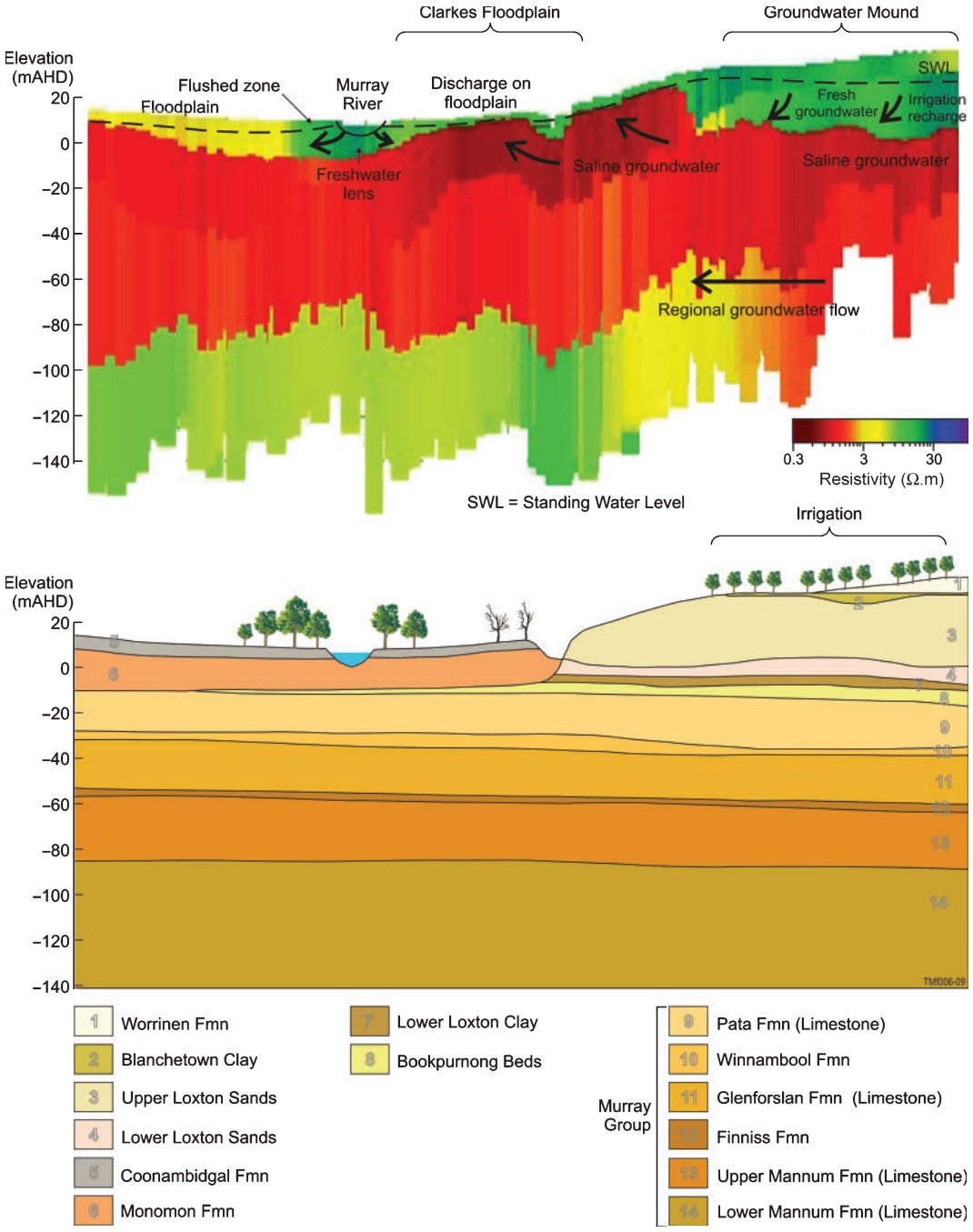

Fig. 7. Resistivity-depth section from the NE–SW flight line (Figure 5*a*) and a corresponding geological section interpreted from regional bore data.

different salinities moving between sub-horizontal sedimentary aquifers of the Murray Group. In plan form, this boundary exhibits a marked spatial variability with significant changes in its depth and regularity (Figure 8). Some distinctive linear features orientated SW to NE suggest that there might be geological control (for example faults) influencing flow between aquifers, although further investigations would be required to confirm this behaviour.

Figure 9 shows the sensitivity analysis, expressed as standard deviation factor on the depth to the bottom of the first layer. Values smaller than 1.5 indicate that a given parameter is resolved (Auken and Christiansen, 2004). This model parameter, like most of the others (not shown), is well resolved throughout the area. At all times we made sure that the inversion fitted the data within measurement noise (normalised data residual <1).

Comparison with single site inversion and with LCI

Against available field data the SCI gave convincing results, mapping conductivity variability both near the surface and at depth. LCI and single-site stitched inversions were also performed on the SkyTEM data (with the same starting model as the SCI). Figure 10 shows average resistivity maps obtained with the LCI and single-site inversion, for the depth interval 2–4 m (the root zone area). The single-site inversion map has a spotted appearance, due to a combination of instabilities in the inversion and data noise. Results from the inversion using the LCI and SCI are similar. However, in some instances the LCI introduces elongated features or artefacts along the flight lines, producing maps with less spatially coherent detail when compared with the results from the SCI (compare Figure 10*a* and *c*). Both the SCI and the LCI bring the conductive layer closer to surface, when compared with the single-site inversion. These results are consistent with available piezometric data. The (relatively) resistive areas in the SCI show a closer correspondence with areas of denser vegetation compared with similar zones identified in results from the single-site inversion and the LCI.

The marked differences between single-site inversion and constrained inversion results (LCI and SCI) are due to the constraints that allow information to migrate between neighbouring soundings in any direction, thereby helping to resolve model parameters that locally would be poorly determined, as in the case of very shallow layers for TEM measurements. It should be noted that the constraints only provide 'suggestions' about neighbouring soundings, based on the expected geological variability in the area. However, these suggestions are accepted (by the SCI) only where they do not contradict the sounding locally (i.e. the data are fitted). This means that if the local sounding data contain significant information locally about a certain model parameter, which is in contrast with the suggestion from the constraints, then the 'suggestion' will not be accepted, and the constraints will be broken. The better resolved the model parameters, the stronger are the suggestions. In this sense, for a poorly resolved part of

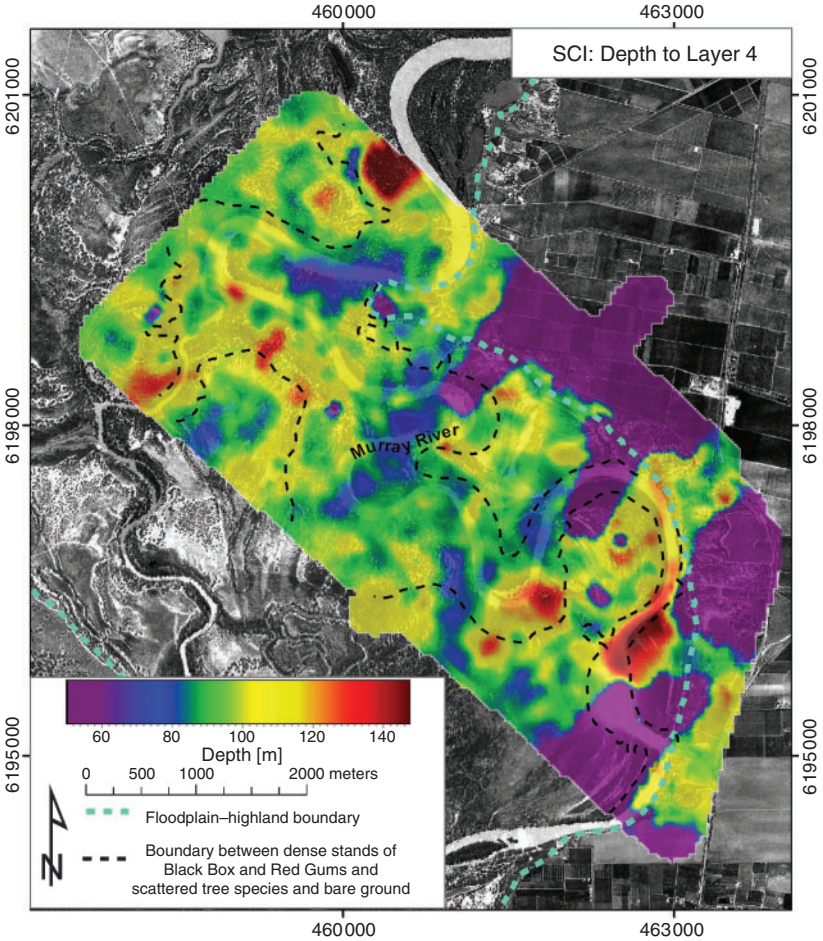

Fig. 8. Depth to the top of layer 4 of the spatially constrained inversion (SCI) inversion from the ground surface.

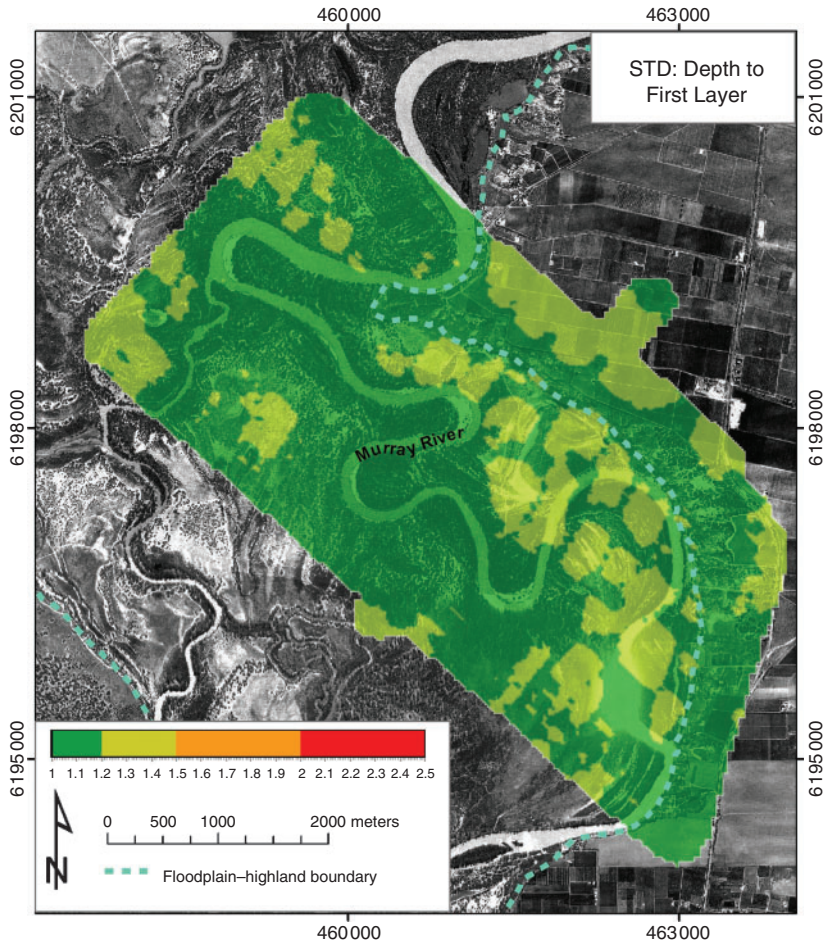

Fig. 9. Standard deviation factor (STD) of depth to first layer from the spatially constrained inversion.

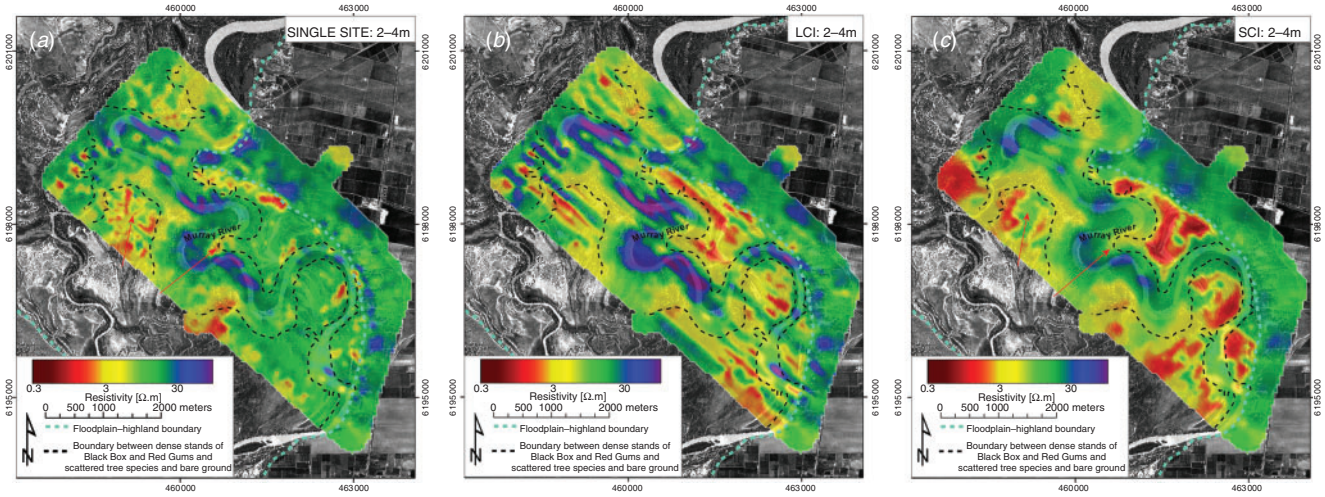

Fig. 10. Comparison between single site (*a*), laterally constrained inversion (LCI) (*b*) and spatially constrained inversion (SCI) (*c*) for resistivity depth interval 2–4 m below the ground surface. Red arrows indicate differences between single site and SCI results in resistive areas.

the model, conductive layers have a higher chance of migrating towards neighbouring soundings than resistive layers do. However, this is not a consequence of the constraints as such, but of the physics of inductive methods, which are more sensitive to conductors than they are to resistors. The SCI produces the most likely result, assuming that the spatial constrains applied reflect the geological variability. If there is information in the data regarding a resistive layer, the SCI will honour it. This behaviour is demonstrated in Figure 10. Careful analysis of the images show several locations (see for example the red arrows) were the SCI produced smoother, larger resistive areas than the single-site inversion did, in accordance with expected hydrogeological variability (which is determined from available borehole information).

The differences between SCI and LCI are due to the constraints being set spatially rather than laterally, which allow the SCI to take full advantage of the spatial coherency in the data. In saline landscapes such as the floodplains of the Lower Murray, the lateral and vertical changes in ground conductivity, caused by changes in groundwater quality, are probably best characterised as being spatially coherent, and slowly varying. It follows therefore, that the SCI will map these variations very effectively. The data were well fitted (more than 95% of the soundings were fitted within noise level) by all three inversion methods.

Conclusions

Based on a 1D forward approximation, the spatially constrained inversion of SkyTEM data produced a credible 3D hydrogeophysical model of the area surveyed, from the very near surface down to greater than 100 m depth. The results confirmed existing knowledge about the hydrogeology, but through the provision of spatial data on groundwater quality, they provided new insights into inter-aquifer connectivity, the relationship between floodplain salinisation and the river, and an enhanced understanding of the link between the irrigation-linked recharge on the highlands, the resulting groundwater mound, and salinisation on the adjacent floodplains.

Over the floodplains the SCI defined a spatially coherent, though variably conductive floodplain with patterns of conductivity varying horizontally and vertically. The most conductive responses are observed in the near surface, particularly on the floodplain (Clark's floodplain) adjacent to highlands, reflecting the distribution of salinity in floodplain soils and groundwater, and confirmed by available borehole data. Results from the inversion provide a basis for better understanding spatial patterns of groundwater evapotranspiration and groundwater quality across the floodplain. Specifically, the SCI identify fine scale variations in the saline groundwater discharge to the river, showing an alternation between losing and gaining groundwater in a stretch of the Murray River broadly understood to be a gaining reach. The presence of a laterally extensive flushed zone adjacent to the river is well defined and in places extends up to 0.5 km away from the river bank. These zones correspond to areas of dense, relatively healthy stands of river red gum (*E. camaldulensis*), black box (*E. largiflorens*) and river cooba (*A. stenophylla*). Zones of high conductivity in the near surface, linked to an accumulation of salts in the floodplain soils, are associated with a complete absence of vegetation or the presence of salt-tolerant plant species.

The localised effect of the salt interception scheme drawing fresh river water into the riverbed sediments appears to be identified in places. The SCI also defines a laterally varying conductivity structure at depth (>100 m) that may reflect a varying groundwater quality in the limestone aquifers of the Murray Group, although this requires confirmation.

Overall, the model parameter sensitivity analysis indicates that the model parameters are well determined. However, we believe that the near-surface results from SkyTEM benefit from the presence of a shallow, extremely good conductor. The definition of variation in the near surface may not be so well defined in the absence of this conductor with the SCI or with the other techniques.

Establishing baseline data on the spatial variation in groundwater conductivity and floodplain salt stores is integral to effective floodplain management in the Murray Basin of South Eastern Australia, and these results suggest data from SkyTEM, when processed using SCI may contribute to achieving that goal.

Acknowledgments

The Bookpurnong SkyTEM data were acquired as part of SA CNRM project #054127: *The application of airborne geophysics to the prediction of groundwater recharge and floodplain salinity management.* TJM's contribution to this study was undertaken as part of that project and their support is acknowledged. This work was also supported by the CSIRO-led Water for a Healthy Country Flagship. The authors also acknowledge the assistance of Andrew Fitzpatrick, Kevin Cahill, Volmer Berens and Mike Hatch in the conduct of work at Bookpurnong. Kevin Cahill was particularly helpful with the presentation of the data.

References

Auken, E., and Christiansen, A. V., 2004, Layered and laterally constrained 2D inversion of resistivity data: *Geophysics*, **69**, 752–761. doi: 10.1190/1.1759461

Auken, E., Christiansen, A. V., Jacobsen, L., and Sørensen, K. I., 2005, Laterally Constrained 1D-Inversion of 3D TEM Data. SAGEEP 2005, Atlanta, USA, EEGS.

Auken, E., Jørgensen, F., and Sørensen, K. I., 2003, Large-scale TEM investigation for groundwater: *Exploration Geophysics*, **34**, 188–194. doi: 10.1071/EG03188

Berens, V., and Hatch, M. A., 2006, In stream geophysics (NanoTEM): a tool to help identify salt accession risk: *Australian Society of Exploration Geophysics Preview*, **120**, 20–25.

Berens, V., White, M. G., Souter, N. J., Jolly, I. D., Holland, K. L., McEwan, K. L., Hatch, M. A., Fitzpatrick, A. D., and Munday, T. J., 2007, Surface Water, Groundwater and Ecological Interactions along the River Murray. A Pilot Study of Management Initiatives at the Bookpurnong Floodplain, South Australia, *Proceedings of the IAH meeting*, 10 pp.

Brown, C. M., and Stephenson, A. E., 1991, Geology of the Murray Basin, Southeastern Australia: BMR Bulletin 235, 430 pp.

Delaunay, B. N., 1934, Sur la sphere vide: *Izvestia Akademii Nauk SSSR, Otdelenie Matematicheskii i Estestvennyka Nauk (Bulletin of Academy of Sciences of the USSR)*, **7**, 793–800.

Huang, H., and Fraser, D. C., 2003, Inversion of helicopter electromagnetic data to a magnetic conductive layered earth: *Geophysics*, **68**, 1211–1223. doi: 10.1190/1.1598113

Jolly, I. D., Holland, K. L., McEwan, K. L., Overton, I. C., White, M. G., Berens, V., and Mensforth, L. J., 2006, The 'Bookpurnong Experiment': will groundwater management and flooding improve the health of the floodplain vegetation? Proceedings International Conference on 'Hydro Eco 2006 – Hydrology and Ecology: The Groundwater/Ecology Connection', Karlovy Vary, Czech Republic, 11–14 September, pp. 305–308.

Lane, R., 2000, Conductive unit parameters: summarising complex conductivity distributions: 70th Meeting, SEG, Calgary, Expanded Abstracts, Volume 1, Section EM4.2, pp. 328–331.

Munday, T. J., Doble, R., Berens, V., and Fitzpatrick, A., 2005, The application of air, ground and 'in river' electromagnetics in the definition of spatial patterns of groundwater induced salt accumulation in a salinising floodplain, lower River Murray, South Australia, *Proceedings of the 19th Annual SAGEEP Symposium*, April 2–6, 2005. SAGEEP, Seattle, USA.

Newman, G. A., Anderson, W. L., and Hohmann, G. W., 1987, Interpretation of transient electromagnetic soundings over three-dimensional structures for the central-loop configuration: *Geophysical Journal of the Royal Astronomical Society*, **89**, 889–914.

Overton, I., and Jolly I., 2004, Integrated Studies of Floodplain vegetation Health, saline groundwater and flooding on the Chowilla floodplain South Australia. CSIRO LW Tech Report 20/04, 169 pp.

Sattel, D., 1998, Conductivity information in three dimensions: *Exploration Geophysics*, **29**, 157–162. doi: 10.1071/EG998157

Sattel, D., 2005, Inverting airborne electromagnetic (AEM) data with Zohdy's method: *Geophysics*, **70**, G77–G85. doi: 10.1190/1.1990217

Sengpiel, K. P., and Siemon, B., 2000, Advanced inversion methods for airborne electromagnetic exploration: *Geophysics*, **65**, 1983–1992. doi: 10.1190/1.1444882

Sørensen, K. I., and Auken, E., 2004, SkyTEM – A new high-resolution helicopter transient electromagnetic system: *Exploration Geophysics*, **35**, 191–199. doi: 10.1071/EG04194

Viezzoli, A., Christiansen, A. V., Auken, E., and Sørensen, K., 2008, Quasi-3D modeling of airborne TEM data by spatially constrained inversion: *Geophysics*, **73**, F105–F113. doi: 10.1190/1.2895521

White, M. G., Berens, V., Souter, N. J., Holland, K. L., McEwan, K. L., and Jolly, I. D., 2006, Vegetation and groundwater interactions on the Bookpurnong floodplain, South Australia, *Proceedings 10th Murray-Darling Basin Groundwater Workshop*, Canberra 18th–20th September 2006.

Wolfgram, P., and Karlik, G., 1995, Conductivity-depth transform of GEOTEM data: *Exploration Geophysics*, **26**, 179–185. doi: 10.1071/EG995179

Yan, W., Howles, S., Howe, B., and Hill, T., 2005, Loxton–Bookpurnong numerical groundwater model 2005. South Australian Government, Department of Water Land and Biodiversity Conservation Report 2005/17. Report prepared for the Murray Darling Basin Commission.

Manuscript received 16 December, 2008; revised manuscript received 2 April, 2009.